Tropospheric chemistry of internally mixed sea salt and organic particles: Surprising reactivity of NaCl with weak organic acids

Alexander Laskin,[1] Ryan C. Moffet,[2,3] Mary K. Gilles,[2] Jerome D. Fast,[4] Rahul A. Zaveri,[4] Bingbing Wang,[1] Pascal Nigge,[2] and Janani Shutthanandan[1]

[1] Chemical imaging analysis of internally mixed sea salt/organic particles collected onboard the Department of Energy (DOE) G-1 aircraft during the 2010 Carbonaceous Aerosols and Radiative Effects Study (CARES) was performed using electron microscopy and X-ray spectro-microscopy. Substantial chloride depletion in aged sea salt particles was observed, which could not be explained by the known atmospheric reactivity of sea salt with inorganic nitric and sulfuric acids. We present field evidence that chloride components in sea salt particles may effectively react with organic acids releasing HCl gas to the atmosphere, leaving behind particles depleted in chloride and enriched in the corresponding organic salts. While formation of the organic salts products is not thermodynamically favored for bulk aqueous chemistry, these reactions in aerosol are driven by high volatility and evaporation of the HCl product from drying particles. These field observations were corroborated in a set of laboratory experiments where NaCl particles mixed with organic acids were found to be depleted in chloride. Combined together, the results indicate substantial chemical reactivity of sea salt particles with secondary organics that has been largely overlooked in the atmospheric aerosol chemistry. Atmospheric aging, and in particular hydration-dehydration cycles of mixed sea salt/organic particles, may result in formation of organic salts that will modify the acidity, hygroscopic, and optical properties of aged particles.

Citation: Laskin, A., R. C. Moffet, M. K. Gilles, J. D. Fast, R. A. Zaveri, B. Wang, P. Nigge, and J. Shutthanandan (2012), Tropospheric chemistry of internally mixed sea salt and organic particles: Surprising reactivity of NaCl with weak organic acids, *J. Geophys. Res.*, *117*, D15302, doi:10.1029/2012JD017743.

1. Introduction

[2] Sea salt aerosol, generated by wave action of seawater, is one of the major sources of naturally produced airborne particles that play an important role in tropospheric chemistry and atmospheric environment [*Keene et al.*, 1998; *Lewis and Schwartz*, 2004]. Atmospheric sea salt particles undergo complex multiphase reactions [*Finlayson-Pitts*, 2003; *Finlayson-Pitts and Hemminger*, 2000; *Rossi*, 2003] that have profound consequences on their evolving physicochemical properties, especially in the areas influenced by anthropogenic emissions. A noticeable depletion of chloride in sea salt particles was

reported in a number of field studies conducted in both polluted and pristine marine environments [*De Bock et al.*, 1994, 2000; *Ebert et al.*, 2000; *Hopkins et al.*, 2008; *Keene*, 1995; *Keene et al.*, 1990; *Kerminen et al.*, 1997, 1998; *Laskin et al.*, 2002, 2005; *Martens et al.*, 1973; *Maskey et al.*, 2011; *McInnes et al.*, 1994; *Mouri and Okada*, 1993; *Mouri et al.*, 1996; *Newberg et al.*, 2005; *Pakkanen*, 1996; *Pio et al.*, 1996; *Pósfai et al.*, 1995, 1994; *Raemdonck et al.*, 1986; *Ro et al.*, 2001; *Sarin et al.*, 2010; *Shaw*, 1991; *Yao and Zhang*, 2012; *Zhao and Gao*, 2008; *Zhuang et al.*, 1999]. The acid displacement reactions of sea salt chlorides with inorganic acids present in the atmosphere are attributed to the chloride depletion that can be expressed in a generalized form:

$$(R1) \qquad ^{\dagger}NaCl\,(aq) + HA\,(aq, g) \leftrightarrow\ ^{\dagger}NaA\,(aq) + HCl\,(aq, g)$$
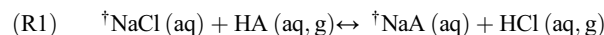
where $^{\dagger}NaCl$ denotes chloride salts of seawater, and HA are atmospheric acids such as HNO_3 (nitric acid), H_2SO_4 (sulfuric acid), and CH_3SO_3H (methanesulfonic acid, MSA). These reactions release volatile HCl(g) to the atmosphere, leaving particles enriched in corresponding salts and depleted in chloride. The majority of field studies report quantitative agreement between depleted chlorine and the combined nitrates, non sea-salt sulfates, and methanesulfonate formed in the particles. However, there are reports that at some geographic locations

---

[1]William R. Wiley Environmental Molecular Sciences Laboratory, Pacific Northwest National Laboratory, Richland, Washington, USA.

[2]Chemical Sciences Division, Lawrence Berkeley National Laboratory, Berkeley, California, USA.

[3]Now at Department of Chemistry, University of the Pacific, Stockton, California, USA.

[4]Atmospheric Science and Global Change Division, Pacific Northwest National Laboratory, Richland, Washington, USA.

Corresponding author: A. Laskin, William R. Wiley Environmental Molecular Sciences Laboratory, Pacific Northwest National Laboratory, Richland, WA 99352, USA. (alexander.laskin@pnl.gov)

Figure 1. G-1 flight path (yellow line) on June 15th during the CARES 2010 study. Colored circles on the flight track correspond to the collection locations of 4 particle samples selected for the microscopy analysis. Corresponding blue, green, beige, and red lines indicate the forward trajectories of particles released at the ocean surface, based on a coupled mesoscale and Lagrangian particle dispersion modeling system, that correspond to the time and space location of the collection aboard the G1.

the chloride deficit in sea salt particles cannot be fully compensated for by the formation of inorganic salts [*Keene et al.*, 1990; *Kerminen et al.*, 1998; *Maskey et al.*, 2011; *Yao and Zhang*, 2012; *Zhao and Gao*, 2008], and additional atmospheric chemistry processes contribute to the chloride depletion. The additional chloride lost can be partially attributed to heterogeneous and interface chemistry with a variety of atmospheric trace species, including OH, HO_2, O_3, NO_2, N_2O_5, and $ClONO_2$ [*Finlayson-Pitts*, 2003] (and references therein). The potential depletion of chloride by reaction with organic acids of anthropogenic origin and corresponding formation of oxalate, malonate, and succinate salts in sea salt particles has been suggested by *Kerminen et al.* [1998]. Potential mechanisms involving HCl(g) displacement by fulvic acids have been proposed and discussed in the literature [*Chameides and Stelson*, 1992, 1993; *Keene et al.*, 1993]. However, the overall role of the organic acids in the chloride depletion remains uncertain and more field and laboratory studies are needed to address this issue.

[3] This work presents results from spectro-microscopy studies that provide quantitative information on the level of chloride depletion in field collected sea salt particles that are internally mixed with anthropogenic organics containing carboxylic acids. Samples were collected during the Carbonaceous Aerosols and Radiative Effects Study (CARES) carried out in June 2010 in Central Valley, California [*Zaveri et al.*, 2012]. The study provided an excellent opportunity to probe atmospherically aged sea salt particles. These particles showed chloride depletion that we attribute to the reactivity of chloride salts with organic acids. Results

from laboratory studies where chloride depletion was detected in artificially prepared mixed NaCl/organic acid particles confirm the possibility of these reactions. The laboratory and field data sets are consistent with one another and indicate a viable pathway for chemical aging and atmospheric processing of sea salt particles that may take place in many geographic areas where marine aerosol interacts with anthropogenic pollutants. The mixing of sea salt particles with anthropogenic secondary organic aerosol (SOA) may facilitate acid displacement reactions that liberate HCl(g) and impact the chemical composition, hygroscopic, and optical properties of particles in ways that were not previously recognized.

2. Experimental Section

2.1. Field-Collected Samples

[4] Particle samples were collected onboard the DOE G-1 aircraft during the research flights conducted at the 2010 CARES study [*Zaveri et al.*, 2012]. Dry airborne particles were deposited on microscopy substrates by a compact time resolved aerosol collector (TRAC) [*Laskin et al.*, 2003, 2006] attached to a common sampling line shared with other instruments. The TRAC is a single stage impactor that deposits particles on a rotating impaction plate containing prearranged substrates. During sample collection, each substrate was exposed for 3 min. The aerodynamic cutoff size (D_{50}) for the TRAC is 0.36 μm. Copper 400 mesh TEM grids coated with Carbon Type-B films (Ted Pella, Inc.) were used for sample collection and analysis. After collection, the samples were sealed and stored pending analysis. In this manuscript, we present data from one flight of the CARES experiment - specifically, the morning flight of June 15th, when sea salt particles contributed to 40–60% of the particle mode in the size range of 0.4–2.5 μm.

[5] Figure 1 shows the G-1 flight path and forward trajectories that are based on mean wind fields and turbulent vertical mixing as simulated by the Weather Research and Forecasting (WRF) model used operationally during CARES [*Fast et al.*, 2011] coupled with a Lagrangian particle dispersion model [*Doran et al.*, 2008]. *Fast et al.* [2011] also presented an evaluation of the WRF simulations and found that simulated wind fields and boundary layer depth were similar to CARES measurements during much of the campaign. In the Lagrangian particle dispersion model, thousands of particles were released over the ocean within a few hundred kilometers of San Francisco and then tracked for the three days prior to June 15th. Particle trajectories shown in Figure 1 are those that intersected the G-1 flight path at the times and locations corresponding to the four sampling episodes selected for detailed particle analyses conveyed in this manuscript. The trajectories indicate that during the time preceding collection, the sampled air mass originated over open areas of the ocean and then passed the San Francisco Bay area prior to arriving to the sampling locations. Based on the meteorological data presented in Figure 1, sea salt particles mixed with anthropogenic pollutants relevant to industrial emissions in the Bay area were expected. The chloride depletion would then be determined by the time that particles had spent in the polluted plume (reaction time). For two sampling episodes, air trajectories indicate a transport time between the Bay area and the sampling location of 8 h. Air trajectories ending at two
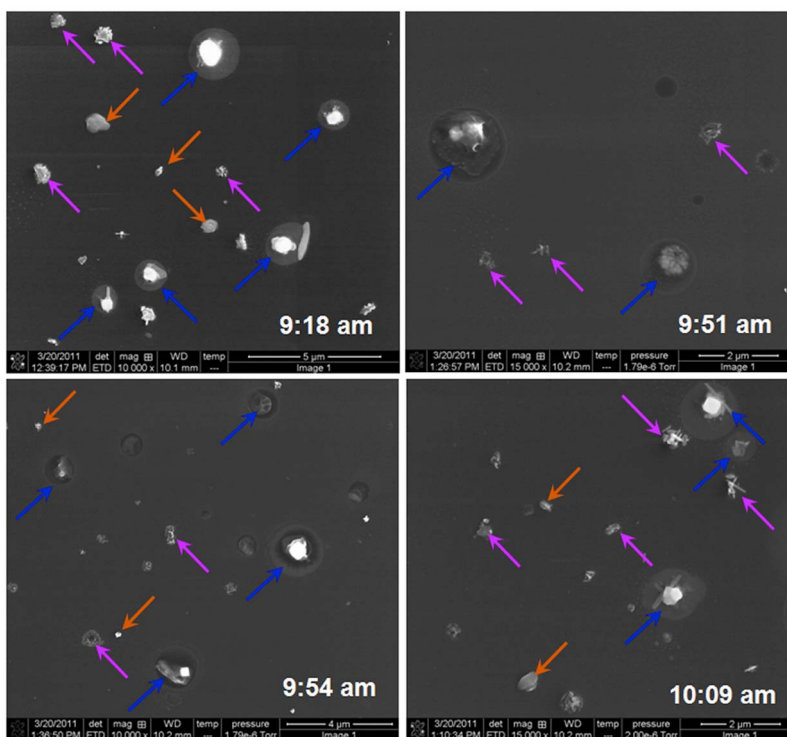
Figure 2. SEM images of representative particles detected at 4 aircraft sampling locations. Blue arrows indicate sea salt particles - irregularly shaped, larger than a micron with NaCl cubic cores and halos of organic material. Magenta arrows indicate sulfate particles with minor contributions of sea salt, and orange arrows indicate ammonium bisulfate/sulfate particles.

additional episodes indicate looping over the San Joaquin Valley and subsequently yielded a longer transport time of 14–25 h. The observed air plume patterns were expected in the area of the study based on meteorological measurements and modeling forecasts [*Fast et al.*, 2011] that were used to design the CARES observation strategy with the scope of examining effects and interactions between biogenic and anthropogenic emissions [*Zaveri et al.*, 2012].

2.2. Laboratory-Generated Samples

[6] Additional CCSEM/EDX particle analysis experiments were preformed on dry particles generated from aqueous solutions of mixed NaCl and organic acids at 1/1 molar ratio and total concentration of 0.5 M. NaCl (99.99% pure), acetic acid (99.7% pure), DL-malic acid (99% pure), malonic acid (99% pure), DL-tartaric acid (99.5% pure), and citric acid (99.5% pure) were obtained from Sigma-Aldrich Co. LLC and used without further purification. Particle samples were prepared in the same manner for all tested mixtures. Liquid particles were nebulized from solutions, and then after being dried in a diffusion dryer, the particles were deposited onto TEM grids placed on the 7th stage (cut-off size, $D_{50} = 0.32$ μm) of the Multi Orifice Uniform Deposition Impactor (MOUDI), model 110-R (MSP, Inc).

2.3. Methods of Particle Analysis

[7] Two complementary analytical techniques were used for particle analysis: computer controlled scanning electron microscopy with energy dispersed analysis of X-rays (CCSEM/EDX), and scanning transmission X-ray
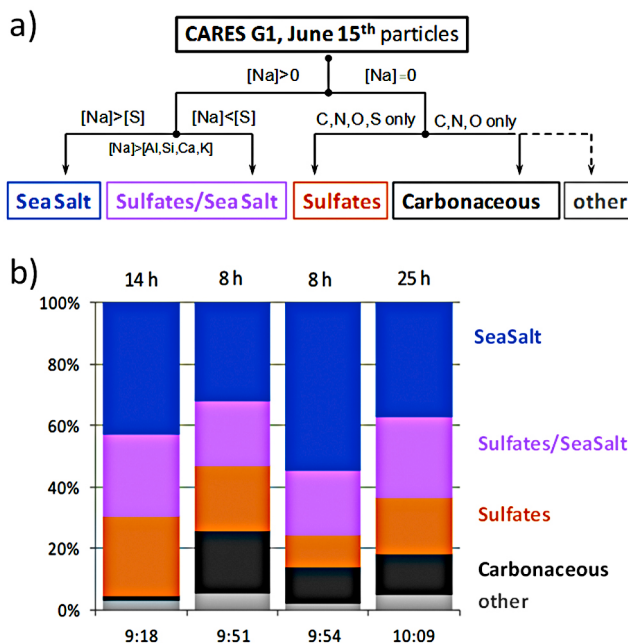

Figure 3. (a) Classification scheme applied to particles from field samples. (b) Stacked column chart diagram of particle classes identified by CCSEM/EDX analysis: "SeaSalt" – blue, mixed "SeaSalt/Sulfate" – magenta, "Sulfates" – orange, "Carbonaceous" – black, "other" – gray.
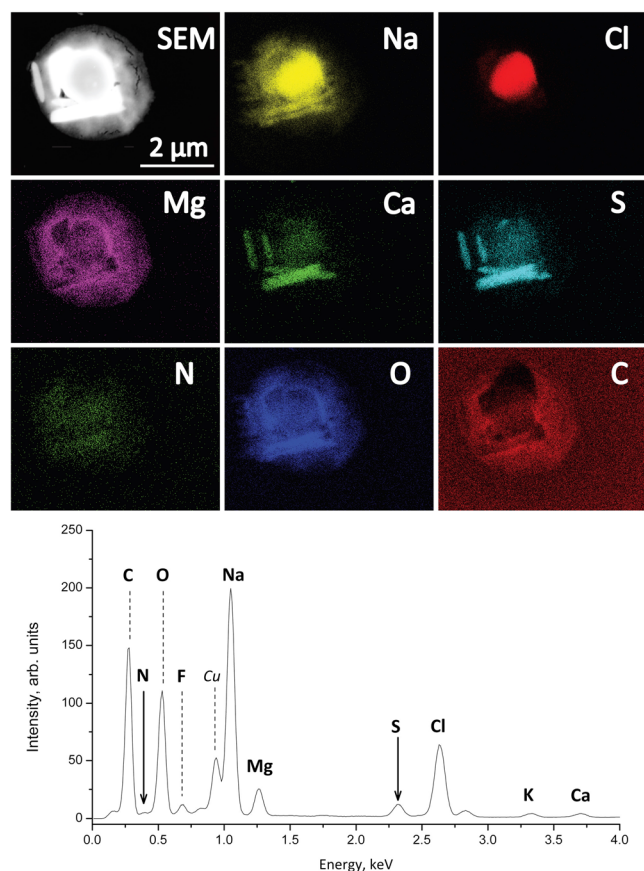
Figure 4. (top) SEM image and EDX elemental maps indicating characteristic internal heterogeneity of aged sea-salt particles from the CARES field study. (bottom) The corresponding EDX spectrum of the particle. Low intensity Cl signals indicate remarkable chloride depletion, and low intensities of N and S suggest only modest formation of nitrates and sulfates. The presence of C, Mg, and Na in the halo area is likely due to formation of organic salts (see text for additional details). *Cu* in the EDX spectrum is a background peak originating from the substrate.

microscopy with near edge X-ray absorption fine structure spectroscopy (STXM/NEXAFS). CCSEM/EDX analysis provides microscopy imaging and quantitative data on elemental composition of individual particles [*Laskin*, 2011; *Laskin et al.*, 2006], while STXM/NEXAFS analysis offers chemical bonding speciation of carbon constituents and an assessment of internal organic/inorganic heterogeneity (mixing state) within individual particles [*Moffet et al.*, 2010a, 2010b].

[8] A FEI Quanta digital field emission gun environmental scanning electron microscope was used in this work. The microscope is equipped with an EDAX X-ray spectrometer with a Si(Li) detector with an active area of 10 mm^2 and an ATW2 window. During CCSEM/EDX operation mode, selected sample areas are inspected and particles are recognized. Then, X-ray spectra are acquired for all detected particles. In this work, particles with an equivalent circle diameter larger than 0.1 μm were measured. The X-ray spectra were acquired for 10 s, at a beam current of 500 pA and an accelerating voltage of 20 kV. Additional details of

the CCSEM/EDX analysis of particles deposited onto carbon coated TEM grids can be found elsewhere [*Laskin et al.*, 2006, and references therein].

[9] STXM/NEXAFS measurements were performed at the carbon K-absorption edge (280–320 eV). STXM instruments at beamlines 5.3.2 and 11.0.2 of the Advanced Light Source at Lawrence Berkeley National Laboratory were used. The intensity of X-rays transmitted through the sample at a fixed energy is measured as the sample is raster scanned to record an image. Sequences of images are acquired at closely spaced energies to record a "stack" of images. NEXAFS spectra from individual pixels or particular regions of interest on the sample image can be extracted from the stack. The absorption through the sample is obtained by converting the signal using the Beer-Lambert law and referencing to the flux measured through a region of substrate free of the sample. The mapping of chemical bonding information in individual particles allows an assessment of particle internal heterogeneity and apportionment of carbon bonding within individual particles [*Moffet et al.*, 2010a].

3. Results and Discussion

[10] Four samples along the flight path of G-1 were selected for particle analysis based on meteorology and basic pollutant measurements obtained from the real-time instrumentation deployed onboard the research aircraft [*Zaveri et al.*, 2012]. Figure 2 shows typical SEM images of characteristic particles commonly present in all four samples. The particles were mostly aged sea salt, sulfur-rich (sulfates), mixed sea salt/sulfates, and carbonaceous particles. Similar to previous studies [*Hoffman et al.*, 2004; *Hopkins et al.*, 2008; *Laskin et al.*, 2002], aged sea salt particles are recognized by their cubic-shaped NaCl cores surrounded by a halo of other components. Ammonium bisulfate/sulfate particles are submicron in size and have a roundish morphology. Sulfate particles internally mixed with sea salts are also mostly submicron in size and have characteristic elongated crystals of sodium sulfate [*Buseck and Pósfai*, 1999].

[11] Figure 3a illustrates the rule-based particle classification scheme that was applied to separate analyzed particles into five major classes. First, all particles containing sodium above the threshold level of 0.5 atomic percent ([Na] > 0) are separated from those without sodium ([Na] = 0). Out of the sodium containing particles, those containing more sodium than any other detected metal are subdivided into two classes: "SeaSalt" - if [Na] > [S], and mixed "SeaSalt/Sulfate" – if [Na] < [S]. The sodium-free particles are subdivided into two additional classes: "carbonaceous" - if quantitative analysis of their X-ray spectra shows the presence of only C, N, and O elements, and "sulfates" – if sulfur is the only other detectable element in addition to C, N, and O. All remaining particles are assigned to a single, nonspecific class of "other" particles. Figure 3b shows the results of this classification for particles detected in the four samples. In each sample, 1000–1500 particles were analyzed and classified. Consistent with the meteorology data predictions, significant populations of sea salt particles were observed in all four samples and comprised up to 40–50% of the total particles by number. Fractions of "sulfates" and mixed "sea salt/sulfate" particles ranged from 10 to 30% between the samples. The fraction of "carbonaceous" particles was less than 15% in all samples.
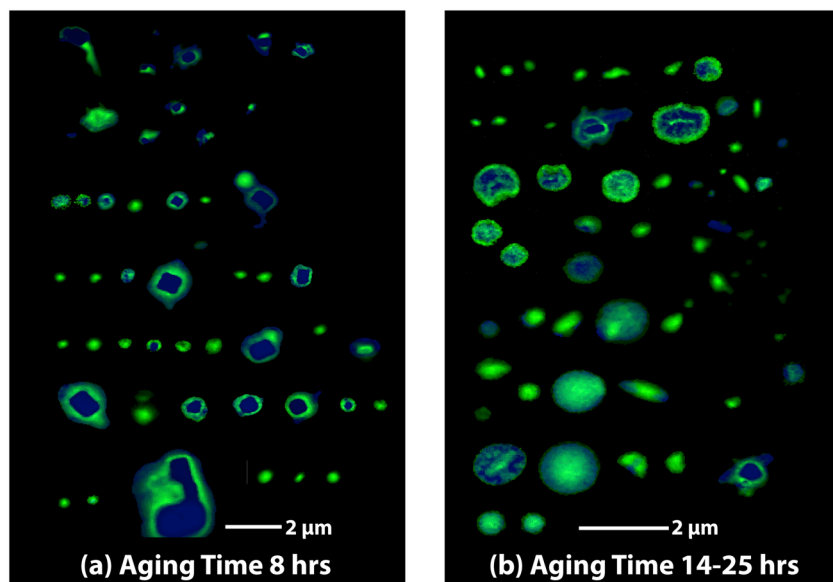
Figure 5. STXM/NEXAFS maps of individual particles detected in samples corresponding to (a) 8 and (b) 14–25 h of transport time as indicated in Figure 1. Areas dominated by organic carbon constituents are green, and inorganic regions are blue. (These panels are compiled from maps of individual particles analyzed in different fields of view and then compiled into a single panel.)

Fractions of "other" particles were only 5%. Particle-type contributions remain consistent in all four samples, and, no trends with shorter (8 h) or longer (14–25 h) transport times (indicated in Figure 1) were observed.

[12] The typical chemical composition of dry aged sea salt particles obtained by SEM/EDX elemental maps for a single representative particle is shown in Figure 4. The observed spatial variations in Na, Mg, Ca, Cl, S, C, N, and O signals indicate formation of different salts outside of the remaining NaCl core, and the substantial enrichment of C-containing constituents in the outer layer (halo area) of the dry particle. The appearance of Mg in the outer layer is consistent with previous studies showing multilayered structures of sea salt particles with highly soluble Mg-containing salts concentrated in the outer layer [*Laskin*, 2011; *Liu et al.*, 2008]. However, in contrast to our previous observations, the Mg map is not well correlated with the corresponding maps of Cl, S, or N that would indicate magnesium chloride, sulfate and nitrate, respectively. On the other hand, the contours and intensity of the Mg map have notable similarities with the C map. The carbon map shows substantial carbonaceous content of the outer layer, which we attribute to the anthropogenic secondary organics that either condensed directly onto the airborne particles from the gas-phase or were formed through the aqueous chemistry of organic precursors during transport to the inland area where the field samples of particles were collected. Figure 4 (bottom) shows an EDX spectrum of the mapped particle. The spectrum shows a significant deficit of Cl, but does not indicate substantial enrichment in S and N that would be associated with potential formation of sulfates and/or nitrates.

[13] STXM/NEXAFS analysis provides specific information on the carbon bonding of the organic material and its internal heterogeneity within individual particles. Figure 5 shows maps of carboxylic acids (green) and inorganic material (blue). This mapping method identifies carboxylic acids based on the intensity of a peak at 288.5 eV, corresponding to C 1s $\rightarrow \pi^*_{COOH}$ transition. Inorganic constituents typically have strong absorbance in the pre-edge (278 eV) whereas organic material will exhibit absorption in the post edge (320 eV); therefore, the pre-edge to post-edge ratio is indicative of the amount of inorganic material relative to organic material. The ratio is then used for mapping of inorganic components in individual particles [*Moffet et al.*, 2010b]. The maps show the presence of carboxylic acids in all analyzed particles. Small homogeneous organic particles may be formed from condensational growth of newly nucleated particles, while larger particles having inorganic cores surrounded by carboxylic acids are a result of condensation of organics onto pre-existing sea salt particles. Figure 5 shows STXM/NEXAFS maps for particles corresponding to 8 (Figure 5a) and 14–25 (Figure 5b) hours of transport time required for the air mass to arrive from the coastal area to the sampling location (see Figure 1). Morphological differences indicative of more extensive processing of sea salt particles at longer transport time can be inferred from the visual comparison of the two panels. Sea salt particles collected at shorter (8 h) transport time generally appear as agglomerates of NaCl cubic crystals (colored by blue) with unstructured halos of organic compounds (colored by green). At longer (14–25 h) transport time sea salt particles are further processed, as indicated by less dominant NaCl cubic cores, and increased areas where organic shells dominate inorganic cores.

[14] A NEXAFS carbon K-edge spectrum of the organic phase characteristic of this study is shown in Figure 6a, and reveals a dominant contribution from carboxylic acids as indicated by the C 1s $\rightarrow \pi^*_{COOH}$ transition at 288.5 eV. A smaller peak corresponding to C 1s $\rightarrow \pi^*_{CO3}$ transition at 290.4 eV in carbonate is also observed. However, the presence of carbonate is typical for marine particles and the corresponding peak has been commonly observed in
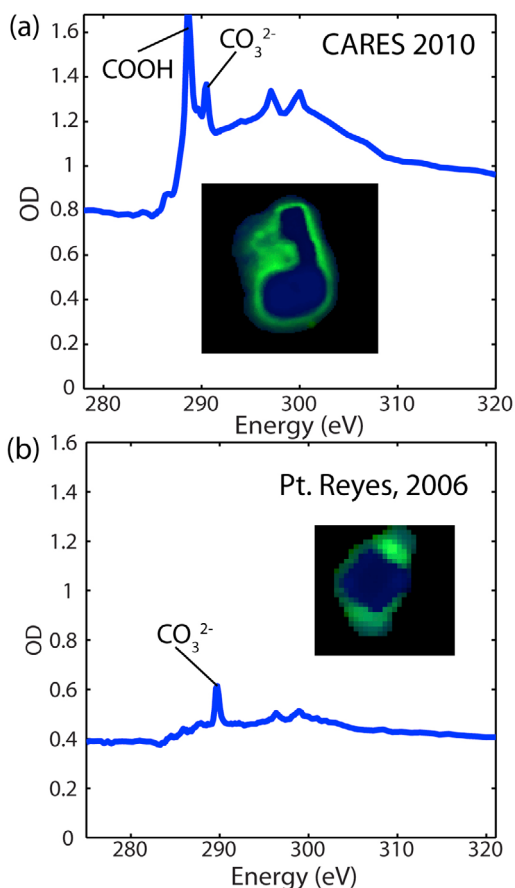
Figure 6. STXM/NEXAFS maps and NEXAFS spectra of organic constituents (green areas) in individual particles characteristic for (a) aged sea salt particles detected in the CARES study and (b) fresh sea salt particles collected in the coastal area of Pt. Reyes National Seashore. Organic material in the aged particle has a characteristic peak at 288.5 eV attributed to the presence of carboxylic acids from anthropogenic sources. A peak at 290.4 eV is attributed to carbonates present in seawater. The carbonates remain unreacted during the aging process and are detected in both fresh and aged particles.

NEXAFS spectra of sea salt particles collected in unpolluted areas. For comparison, Figure 6b shows a map and typical organic phase NEXAFS spectrum for fresh sea salt particles collected during a previous field study north of San Francisco, at the Point Reyes National Seashore [*Hopkins et al.*, 2008]. Comparison of the NEXAFS spectra shows that the carboxyl functionality is very minor in the fresh sea salt, and is well pronounced in the anthropogenic organic material detected in the aged sea salt particles described in this study. The difference in absorption between the post-edge (320 eV) and the pre-edge (280 eV) is an indication of the amount of carbonaceous material present in the particles. It is clear that the particles collected in the CARES study contain significantly more carbon.

[15] Figure 7 shows the experimentally measured elemental ratios of Cl/(Na+0.5Mg) (Figure 7, top) and (Cl+N+0.5S)/(Na+0.5Mg) (Figure 7, bottom) for all particles (~4000 total) from this study assigned to the "sea salt" class.

The dashed line in Figure 7 (top) indicates the characteristic ratio expected in fresh sea salt particles, and the dashed line in Figure 7 (bottom) is the ratio expected if chloride is entirely displaced by nitrates and sulfates. Particles from the four different samples are marked with different colors, and show fairly similar results without consistent differences between the samples. The plots show that the majority of particles are either substantially or even completely depleted of chlorine, yielding low Cl/(Na+0.5Mg) ratios with a size dependence indicative of more extensive processing of smaller particles. If all missing chloride was quantitatively balanced by formation of nitrate and sulfates exclusively, a modified (Cl+N+0.5S)/(Na+0.5Mg) ratio assessed for individual particles would be close to unity. However, the vast majority of the corresponding (Cl+N+0.5S)/(Na+0.5Mg) ratios are only 30–40% of the value that would correspond to complete and quantitative formation of nitrates and sulfates. Therefore, additional chemical reactions must contribute significantly (60–70%) to the observed chlorine depletion. The results of STXM/NEXAFS (Figures 5 and 6) and SEM/EDX (Figure 4) mapping analysis suggest that carboxylic acid components of the condensed organic material may evoke the possibility of additional acid-displacement reactions that would liberate HCl(g) to the atmosphere. This would be accompanied by the formation of corresponding organic salts of magnesium and sodium inside particles.
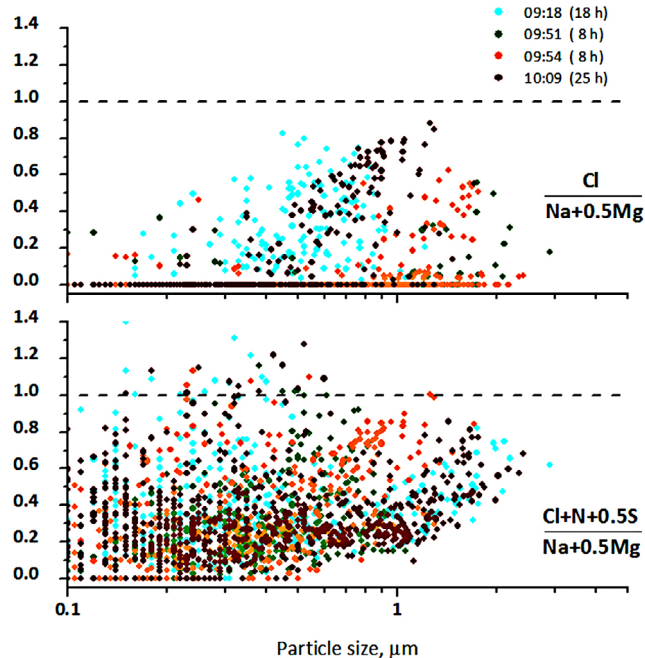

Figure 7. Elemental ratios measured by CCSEM/EDX in particles (~4000 total) assigned to the "sea salt" class from all four samples. Each sample is color coded for the transport time. (top) Cl/(Na+0.5Mg) ratios, the dashed line of ratio = 1 corresponds to unreacted sea salt. (bottom) Ratios of (Cl+N+0.5S)/(Na+0.5Mg), the dashed line of ratio = 1 corresponds to aged sea salt particles with chloride quantitatively displaced by only nitrate and sulfate. These plots indicate that chloride depletion is substantial and cannot be accounted for by the reactions with atmospheric nitric and sulfuric acids.
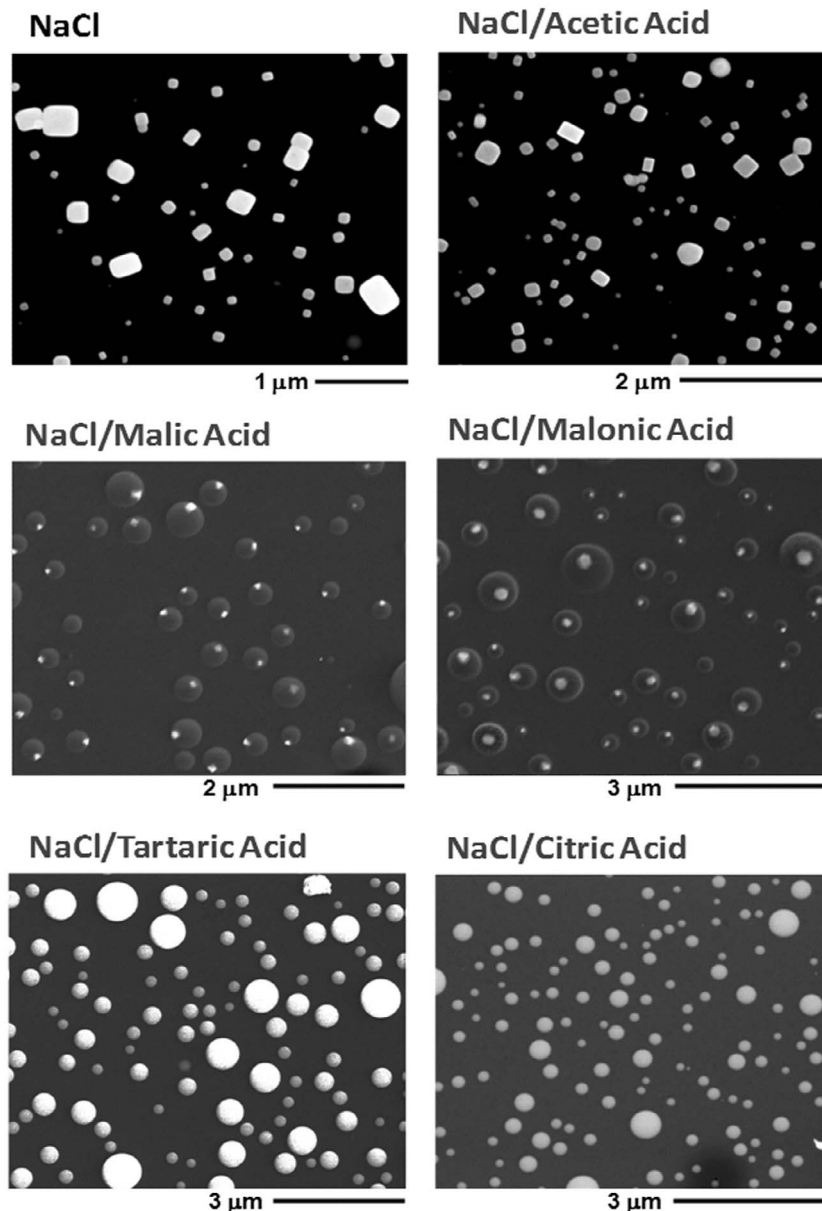
Figure 8. SEM images illustrating morphology and the internal heterogeneity of mixed NaCl/organic acids particles. NaCl particles are shown for comparison.

[16] To evaluate the plausibility of chloride depletion by carboxylic acids, laboratory tests on aerosolized particles of mixed NaCl/organic acid composition (1/1 molar ratio) were performed. Particles were atomized from aqueous solutions of known concentrations. The atomized particles were first dried in the diffusion drier, followed by deposition on substrates, and CCSEM/EDX particle analysis. Figure 8 shows SEM images of particles observed in these tests along with a control test where pure NaCl particles were generated, deposited, and analyzed following the same experimental protocol. With the exception of mixed NaCl/acetic acid particles, the particle morphologies in all other samples are unique and remarkably different from pure NaCl. Mixed NaCl/malic acid and NaCl/malonic acid particles have characteristic core/shell round morphologies. In these two cases, the amorphous organic salt forms outer shells that are largely electron transparent, and are seen as relatively dark areas while the remaining NaCl residues appear as bright cores. NaCl cores are located in the center of NaCl/malonic acid particles, while NaCl/malic acid particles can be described as partially engulfed structures, where NaCl residues are adjacent to the edge of the organic salt. Mixed NaCl/tartaric acid and NaCl/citric acid particles show round homogeneous morphology typical for amorphous or glassy materials. Mixed NaCl/acetic acid particles have morphologies very similar to cubic structures of pure NaCl crystals; however, their edges are more rounded.

[17] Figure 9 summarizes results of the CCSEM/EDX elemental analyses of individual NaCl/organic acid particles prepared in the test experiments. The individual panels show elemental Cl/Na ratios obtained from the quantitative
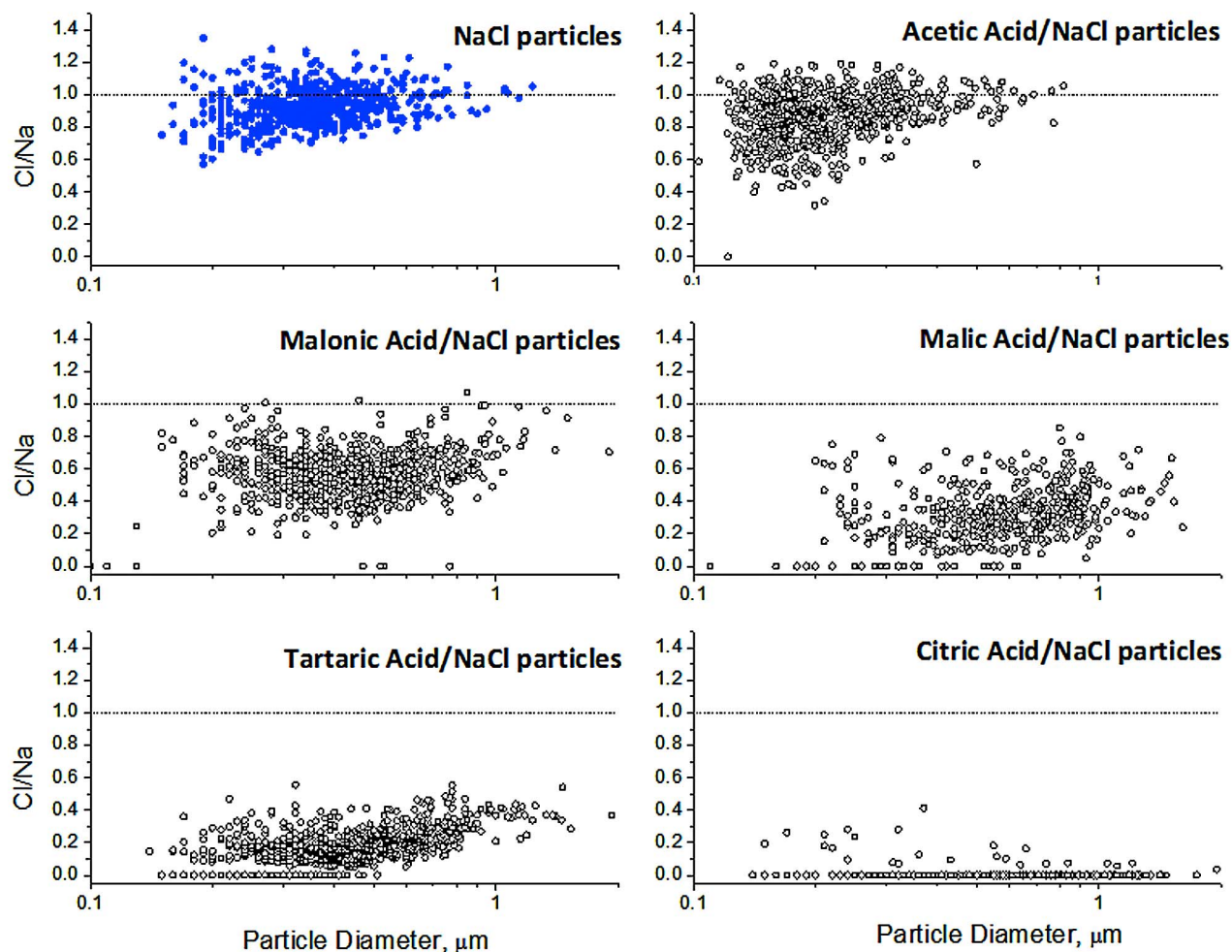
Figure 9. Values of Cl/Na ratios measured by CCSEM/EDX in dry residues of NaCl, and mixed organic acid/NaCl (1/1 molar ratio) particles. Values of Cl/Na below unity (dashed lines) indicate Cl depletion by organic acids.

assessment of EDX spectra of 500–1000 particles in a size range of 0.15–2 μm for each of the tested compositions. As a reference, the first panel shows Cl/Na ratios measured for pure NaCl particles generated and deposited on the substrates following the same procedure. The dashed horizontal lines show the nominal ratio of Cl/Na = 1. Within experimental scatter, the measured values of Cl/Na closely match the nominal unity value for the pure NaCl particles. In sharp contrast, the elemental analysis of mixed NaCl/organic acid particles showed chloride depletion in all other experiments. However, the extent of the observed chloride depletion varied. The lowest (ca. 10–20%) depletion was observed for NaCl/acetic acid particles. Mixed particles of NaCl/malonic acid composition indicate chloride depletion in a range of 40–60%. Higher values of 60–90% were typical for NaCl/malic acid and NaCl/tartaric acid particles, and nearly complete depletion of chloride is evident in mixed NaCl/citric acid particles.

[18] We attribute the observed depletion of chloride to the acid displacement reactions with a general formula analogous to R1 where HCl(g) is displaced by organic acids, specified as HA(org). Initially, this assumption may seem counterintuitive based on general chemistry and reaction

equilibriums based on relative acidities (dissociation) of HCl and HA(org) in dilute aqueous solutions. Table 1 lists solubility, acid dissociation constants (K_{a1}), and Henry's law constants (K_H) for these acids. In view of the K_{a1} values listed in the table, for the system of mixed NaCl/citric acid aqueous (deliquesced) particles, the concentration of undissociated HCl would be a factor of 1.2×10^{10} lower than the undissociated HA(citric acid). As water is removed from drying particles, they become more concentrated in all the components, and at some point HCl and HA(citric acid) begin to evaporate while sodium citrate and NaCl start to precipitate. Corresponding K_H values indicate that the equilibrium gas-phase concentration of HCl can be a factor of 1×10^{19} higher than that of HA(citric acid). Therefore, for the aerosolized particles at gas-particle equilibrium, the gas-phase release of HCl(g) will control the direction of reaction, R1, in the case of mixed NaCl/citric acid particles. During the drying process, undissociated HCl would undergo continuous degassing (effervescence), leaving dried particles devoid of chloride and enriched in citrate salt, which is consistent with our experimental observations (Figure 9). In contrast, for the case of mixed NaCl/acetic acid particles the

Table 1. Physicochemical Properties of Acids Discussed in This Work

Acids	Molecular Formula	Molar Mass (g mol^{-1})	Solubility in Water[a] (g L^{-1}, at 20°C)	Acidity K_{a1}(aq)[a]	Henry's Law Constant, $k_{H.}$[b] (M/atm, at 25°C)
Hydrochloric	HCl	36.46	720	$>1 \times 10^7$	$<2 \times 10^{-1}$
Sulfuric	H_2SO_4	98.08	miscible	$>1 \times 10^3$	$>1 \times 10^7$
Methanesulfonic	CH_3SO_3H	96.11	miscible	7.9×10^1	8.2×10^{11}
Nitric	HNO_3	63.01	miscible	$>2 \times 10^1$	$>2 \times 10^5$
Acetic	$C_2H_4O_2$	60.05	miscible	1.8×10^{-5}	$>4.1 \times 10^3$
Malonic	$C_3H_4O_4$	104.06	miscible	1.5×10^{-3}	4.0×10^8
Malic	$C_4H_6O_5$	134.09	558	3.9×10^{-4}	2.0×10^{13}
Tartaric	$C_4H_6O_6$	150.09	1330	1.0×10^{-3}	1.0×10^{18}
Citric	$C_6H_8O_7$	192.12	730	8.4×10^{-4}	2.0×10^{18}

[a]Data from *Haynes* [2011].
[b]Data from R. Sander, Compilation of Henry's Law Constants for Inorganic and Organic Species of Potential Importance in Environmental Chemistry (Version 3), 1999, http://www.henrys-law.org.

situation is different, the equilibrium gas-phase concentration of HCl would be only by a factor of 2×10^4 higher than that of HA(acetic acid), and is insufficient to overcome the equilibrium limit of HCl and HA(acetic acid) in the aqueous phase which favors HA(acetic acid) by a factor of 5×10^{11}. In this case, upon drying, evaporation of HA(acetic acid) from particles exceeds evaporation of HCl, and dry particles become devoid in acetate and enriched in chloride, which is also in agreement with our observations (Figure 9). In three other cases of mixed NaCl/organic acids particles, these considerations indicate a reasonable (within an order of magnitude) balance between differences in the equilibrium gas-phase and aqueous-phase concentrations of HCl and HA(organic acid) and therefore explain partial chloride depletion observed in these cases (Figure 9). Notably, the same arguments apply to the atmospherically relevant reactivity of NaCl particles with HNO_3 and H_2SO_4, and CH_3SO_3H acids. Considering the acidity argument alone, formation of HCl(aq) by the acid displacement reaction R1 is not thermodynamically favored in bulk aqueous solutions because HCl is the strongest acid of all acids discussed here (see Table 1). However, in airborne particles the equilibrium of reaction R1 can be shifted to the right because of the efficient evaporation of HCl(g) from the particle surface, considering high surface-to-volume ratios characteristic for aerosols.

[19] We note that both CCSEM/EDX and STXM/NEX-AFS analyses detect the composition of dry particles, which may not be identical to the composition of the airborne particles at atmospherically relevant RH. Prior to analysis, particles are dried in the sampling line, inside of the impactor upon collection, and finally either in the vacuum chamber of SEM or in the He filled chamber of STXM during the analysis. Therefore, we cannot determine what fraction of HCl was released in the atmosphere, and what fraction of HCl was lost during sampling and analysis. The field data presented in this manuscript indicates the terminal composition of particles when depletion of chloride has been completed to the maximum extent achieved in dry particles. Analysis of particle composition and the gas-particle partitioning of HCl at specific ambient conditions (RH, temperature, pressure, and particle concentration) of our field study is not a trivial task because of insufficient information on detailed chemical characterization of ambient organic acids and their corresponding concentrations. However, gas-particle partitioning of HCl at ambient conditions can be qualitatively assessed using an E-AIM community model for

calculating gas/liquid/solid partitioning in aerosol systems (http://www.aim.env.uea.ac.uk/aim/aim.php [*Clegg and Seinfeld*, 2006a, 2006b]) when applied for a simplified system of mixed NaCl/malonic acid particles. Figure 10 shows the Cl/Na ratio in condensed phase (aqueous ions and solids) calculated at different RH values for particles containing water, NaCl and malonic acid at 1:1 molar ratio, at equilibrium with an atmosphere at P = 1 atm and 298.15 K (additional details of input data are summarized in the auxiliary material).[1] The ratios are calculated for atmospheric concentrations of NaCl particles in a range of $1-10^3$ $\mu g \cdot m^{-3}$ that represents a typical range of airborne sea salt concentrations [*Lewis and Schwartz*, 2004]. Solid lines indicate modeling results calculated for aqueous (thick lines) and metastable, supersaturated

---

[1]Auxiliary materials are available in the HTML. doi:10.1029/2012JD017743.
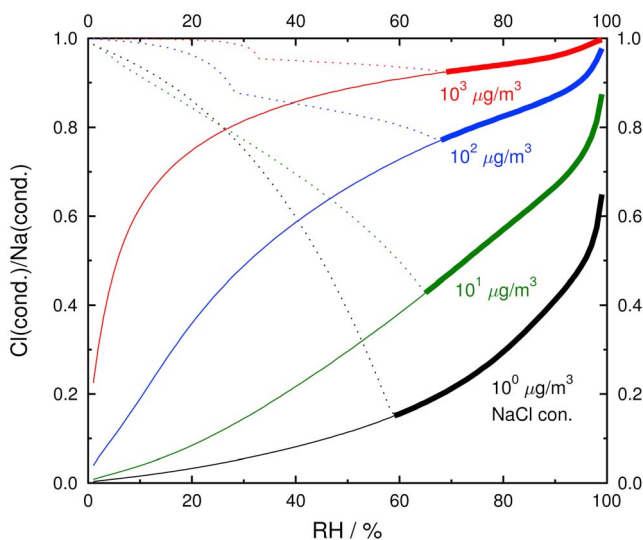
Figure 10. Condensed phase ratios of Cl/Na in mixed NaCl/malonic acid (1/1 molar ratio) particles calculated using E-AIM model for four airborne concentrations of NaCl particles, as indicated by the legends, respectively. Solid lines indicate equilibrium ratios calculated for aqueous (thick lines) and metastable (thin lines) particles. Dotted lines indicate calculations with solid phases of malonic acid and NaCl allowed to form. (See text for additional discussion.)

particles (thin lines), with formation of the solid phases disabled in the model input. Dotted lines correspond to the cases when solid phases of NaCl and malonic acid were allowed to form. As indicated by the modeling results, the chloride depletion in mixed NaCl/malonic acid particles is highly dependent on atmospheric concentration of aerosol with the highest depletion extent predicted for the most diluted system of 1 $\mu g \cdot m^{-3}$. Notably, even for deliquesced particles at 80% RH, the Cl/Na ratio can be as low as 0.3, for the lowest aerosol concentration of 1 $\mu g \cdot m^{-3}$ (black line); and for the highest concentration of 10^3 $\mu g \cdot m^{-3}$ the calculated ratio of Cl/Na is at the level of 0.9 (red line). Considering metastable phase of drying NaCl/malonic acid (1:1) particles at 30–50% RH, Cl/Na ratios of 0.2–0.5 are predicted for a mid range (10–100 $\mu g \cdot m^{-3}$) of typical sea salt concentrations (green and blue lines, respectively). The present version of the E-AIM model assumes only malonic acid itself as its solid phase, and does not consider formation of malonate and mixed malonate/chloride salts. As a result, modeling results with the solid phase of malonic acid show increasing Cl/Na ratio once the concentration of malonic acid reaches saturation at low RH, as marked by dotted lines in Figure 10. More detailed modeling analysis of the HCl gas-particle partitioning at low RH would require explicit speciation of additional solid phases which lies beyond the scope of this work. Nevertheless, based on the modeling results applicable to the cases of gas-aqueous phase partitioning only (thick solid lines), we conclude that chemical reactivity of mixed NaCl/malonic acid particles, and the resulting HCl gas-particle partitioning are not limited only to dry particles, but are also pertinent to deliquesced particles aerosolized at atmospherically relevant concentrations. Other water soluble organic acids may have similar effects on the composition of mixed sea salt/organic acid particles with important implications for atmospheric chemistry of wet sea salt spray at high relative humidity typical for marine and coastal air masses.

[20] Modeling results presented in Figure 10 assume a closed thermodynamic system, and imply reversibility of gas-particle partitioning for HCl and other species involved, which is not necessarily true for the real atmospheric system. For instance, HCl(g) released from sea salt particles may be undergo gas-phase reaction with OH radicals yielding reactive Cl-atoms [*Riedel et al.*, 2012], that in turn can react rapidly with organics. In addition, released HCl(g) may participate in heterogeneous reactions with co-existing particles such as mineral dust, where the latter may act as irreversible sink for HCl. Previous field observations and the transport modeling study of *Sullivan et al.* [2007] provided strong evidence for this type of chemistry in externally mixed sea-salt and mineral dust aerosol that was attributed to the consequences of the sulfate formation/chloride depletion in sea salt [*Sullivan et al.*, 2007]. Based on the data presented here, presence of organic acids in sea salt droplets may yield the same result, where released HCl(g) would alter composition of co-existing dust particles and atmospheric budgets of gas-phase species as well.

[21] Water soluble low volatility organic acids present in aged sea salt particles containing nitrates may additionally alter gas-particle partitioning of HNO_3 in a similar fashion to the HCl volatilization, but likely at lower extent. Figure S1 of the auxiliary information file shows equilibrium concentrations calculated for $NaNO_3$/malonic acid (1:1 molar ratio)

particles and indicate potential volatilization of HNO_3(g) at the level of 50% at aerosol concentration of 1 $\mu g \cdot m^{-3}$. Again, the reaction is driven by relatively high volatility of HNO_3(g) and its evaporation through particle surface. Contrary, equilibrium concentrations calculated for $0.5Na_2SO_4$/malonic acid particles (shown on the same plot, auxiliary material Figure S1) indicate no changes in particle composition, which is consistent with very low volatility of sulfuric acid. Given potential volatilization of HNO_3(g) upon reaction with organic acids, it might be possible that both chloride and nitrate were depleted from the aged sea salt particles reported in this study as a result of similar acid-displacement reactions.

4. Conclusions and Atmospheric Implications

[22] This combined laboratory study of field collected and laboratory generated particles suggests that atmospheric particles containing sea salt and organic acids exhibit substantial acid-displacement reactivity upon drying. Low volatility carboxylic acids are inherent constituents of SOA formed from both biogenic and anthropogenic precursors, and therefore the composition of mixed NaCl/SOA particles will be likely affected by the same reaction processes. These reactions liberate HCl(g) and promote the formation of organic salts in the particle phase. In the atmospheric environment, the released HCl(g) may result in consecutive acidification of co-existing neighboring particles, and trigger additional acid-base reactions, especially with alkaline components of mineral dust or fly ash particles [*Al-Hosney et al.*, 2005; *Chen et al.*, 2012; *Cwiertny et al.*, 2008; *Moffet et al.*, 2008; *Prince et al.*, 2008; *Sullivan et al.*, 2007]. Formation and precipitation of organic salts will modify the internal composition of particles and, in turn, may inhibit acid-catalyzed reactions relevant to SOA aging, alter particle viscosity, their hygroscopic and optical properties, and propensity to serve as cloud condensation and ice nuclei. Due to the high abundances of sea salt and SOA, and common mixing between them, the acid displacement reactions may play a significant role in areas where marine aerosol combines with either anthropogenic or biogenic organic emissions. Currently, this chemistry and the associated changes in particle properties are not considered at even the phenomenological level by any modeling efforts. Data presented here warrant additional examinations of the chloride deficit in marine particles induced by the presence of organic acids, with an ultimate goal to include these processes into the atmospheric chemistry models applicable for coastal urban regions. The coarse spatial resolution ($\Delta x \sim 100$ km) currently employed by global climate models do not allow an accurate representation of the evolving chemistry in the vicinity of coastal regions. However, as regional-scale ($\Delta x \sim 10$ km) climate assessments become routine in the future (as a result increased computational resources), a more complete representation of chemistry associated with mixing marine and continental air masses is needed.

References

Al-Hosney, H. A., S. Carlos-Cuellar, J. Baltrusaitis, and V. H. Grassian (2005), Heterogeneous uptake and reactivity of formic acid on calcium carbonate particles: A Knudsen cell reactor, FTIR and SEM study, *Phys. Chem. Chem. Phys.*, 7(20), 3587–3595, doi:10.1039/b510112c.

Buseck, P. R., and M. Posfai (1999), Airborne minerals and related aerosol particles: Effects on climate and the environment, *Proc. Natl. Acad. Sci. U. S. A.*, 96(7), 3372–3379, doi:10.1073/pnas.96.7.3372.

Chameides, W. L., and A. W. Stelson (1992), Aqueous-phase chemical processes in deliquescent sea-salt aerosols: A mechanism that couples the atmospheric cycles of S and sea salt, *J. Geophys. Res.*, 97(D18), 20,565–20,580, doi:10.1029/92JD01923.

Chameides, W. L., and A. W. Stelson (1993), Reply, *J. Geophys. Res.*, 98(D5), 9051–9054, doi:10.1029/93JD00310.

Chen, H., A. Laskin, J. Baltrusaitis, M. M. Scherer, and V. H. Grassian (2012), Coal combustion fly ash as a source of iron in atmospheric dust, *Environ. Sci. Technol.*, 46(4), 2112–2120, doi:10.1021/es204102f.

Clegg, S. L., and J. H. Seinfeld (2006a), Thermodynamic models of aqueous solutions containing inorganic electrolytes and dicarboxylic acids at 298.15 K. I. The acids as non-dissociating components, *J. Phys. Chem. A*, 110, 5692–5717, doi:10.1021/jp056149k.

Clegg, S. L., and J. H. Seinfeld (2006b), Thermodynamic models of aqueous solutions containing inorganic electrolytes and dicarboxylic acids at 298.15 K. II. Systems including dissociation equilibria, *J. Phys. Chem. A*, 110, 5718–5734, doi:10.1021/jp056150j.

Cwiertny, D. M., J. Baltrusaitis, G. J. Hunter, A. Laskin, M. M. Scherer, and V. H. Grassian (2008), Characterization and acid-mobilization study of iron-containing mineral dust source materials, *J. Geophys. Res.*, 113, D05202, doi:10.1029/2007JD009332.

De Bock, L. A., H. Van Malderen, and R. E. Van Grieken (1994), Individual aerosol-particle composition variations in air masses crossing the North Sea, *Environ. Sci. Technol.*, 28(8), 1513–1520, doi:10.1021/es00057a021.

De Bock, L. A., P. E. Joos, K. J. Noone, R. A. Pockalny, and R. E. Van Grieken (2000), Single particle analysis of aerosols, observed in the marine boundary layer during the Monterey Area Ship Tracks Experiment (MAST), with respect to cloud droplet formation, *J. Atmos. Chem.*, 37(3), 299–329, doi:10.1023/A:1006416600722.

Doran, J. C., J. D. Fast, J. C. Barnard, A. Laskin, Y. Desyaterik, and M. K. Gilles (2008), Applications of Lagrangian dispersion modeling to the analysis of changes in the specific absorption of elemental carbon, *Atmos. Chem. Phys.*, 8, 1377–1389, doi:10.5194/acp-8-1377-2008.

Ebert, M., S. Weinbruch, P. Hoffmann, and H. M. Ortner (2000), Chemical characterization of North Sea aerosol particles, *J. Aerosol Sci.*, 31(5), 613–632, doi:10.1016/S0021-8502(99)00549-2.

Fast, J. D., et al. (2011), Transport and mixing patterns over Central California during the Carbonaceous Aerosol and Radiative Effects Study (CARES), *Atmos. Chem. Phys. Discuss.*, 11, 29,949–30,008, doi:10.5194/acpd-11-29949-2011.

Finlayson-Pitts, B. J. (2003), The tropospheric chemistry of sea salt: A molecular-level view of the chemistry of NaCl and NaBr, *Chem. Rev.*, 103(12), 4801–4822, doi:10.1021/cr020653t.

Finlayson-Pitts, B. J., and J. C. Hemminger (2000), Physical chemistry of airborne sea salt particles and their components, *J. Phys. Chem. A*, 104(49), 11,463–11,477, doi:10.1021/jp002968n.

Haynes, W. M. (Ed.) (2011), *CRC Handbook of Chemistry and Physics*, 92nd ed., CRC, Boca Raton, Fl.

Hoffman, R. C., A. Laskin, and B. J. Finlayson-Pitts (2004), Sodium nitrate particles: Physical and chemical properties during hydration and dehydration, and implications for aged sea salt aerosols, *J. Aerosol Sci.*, 35(7), 869–887, doi:10.1016/j.jaerosci.2004.02.003.

Hopkins, R. J., Y. Desyaterik, A. V. Tivanski, R. A. Zaveri, C. M. Berkowitz, T. Tyliszczak, M. K. Gilles, and A. Laskin (2008), Chemical speciation of sulfur in marine cloud droplets and particles: Analysis of individual particles from the marine boundary layer over the California current, *J. Geophys. Res.*, 113, D04209, doi:10.1029/2007JD008954.

Keene, W. C. (1995), Inorganic Cl cycling in the marine boundary layer: A review, in *Naturally Produced Organohalogens*, edited by A. Grimvall

and E. W. B. de Leer, pp. 363–441, Kluwer Acad., Norwell, Mass., doi:10.1007/978-94-011-0061-8_34.

Keene, W. C., A. A. P. Pszenny, D̄. J. Jacob, R. A. Duce, J. N. Galloway, J. J. Schultz-Tokos, H. Sievering, and J. F. Boatman (1990), The geochemical cycling of reactive chlorine through marine troposphere, *Global Biogeochem. Cycles*, 4(4), 407–430, doi:10.1029/GB004i004p00407.

Keene, W. C., D. J. Jacob, A. A. P. Pszenny, R. A. Duce, J. J. Schultztokos, and J. N. Galloway (1993), Comment on "Aqueous-phase chemical processes in deliquescent sea-salt aerosols: A mechanism that couples the atmospheric cycles of S and sea-salt," *J. Geophys. Res.*, 98(D5), 9047–9049, doi:10.1029/93JD00259.

Keene, W. C., R. Sander, A. A. P. Pszenny, R. Vogt, P. J. Crutzen, and J. N. Galloway (1998), Aerosol pH in the marine boundary layer: A review and model evaluation, *J. Aerosol Sci.*, 29(3), 339–356, doi:10.1016/S0021-8502(97)10011-8.

Kerminen, V. M., T. A. Pakkanen, and R. E. Hillamo (1997), Interactions between inorganic trace gases and supermicrometer particles at a coastal site, *Atmos. Environ.*, 31(17), 2753–2765, doi:10.1016/S1352-2310(97)00092-7.

Kerminen, V. M., K. Teinila, R. Hillamo, and T. Pakkanen (1998), Substitution of chloride in sea-salt particles by inorganic and organic anions, *J. Aerosol Sci.*, 29(8), 929–942, doi:10.1016/S0021-8502(98)00002-0.

Laskin, A. (2011), Electron beam analysis and microscopy of individual particles, in *Fundamental Applications in Aerosol Spectroscopy*, edited by R. Signorell and J. P. Reid, pp. 463–491, Taylor and Francis, Philadelphia, Pa., doi:10.1201/b10417-23.

Laskin, A., M. J. Iedema, and J. P. Cowin (2002), Quantitative time-resolved monitoring of nitrate formation in sea salt particles using a CCSEM/EDX single particle analysis, *Environ. Sci. Technol.*, 36(23), 4948–4955, doi:10.1021/es020551k.

Laskin, A., M. J. Iedema, and J. P. Cowin (2003), Time-resolved aerosol collector for CCSEM/EDX single-particle analysis, *Aerosol Sci. Technol.*, 37(3), 246–260, doi:10.1080/02786820300945.

Laskin, A., M. J. Iedema, A. Ichkovich, E. R. Graber, I. Taraniuk, and Y. Rudich (2005), Direct observation of completely processed calcium carbonate dust particles, *Faraday Discuss.*, 130, 453–468, doi:10.1039/b417366j.

Laskin, A., J. P. Cowin, and M. J. Iedema (2006), Analysis of individual environmental particles using modern methods of electron microscopy and X-ray microanalysis, *J. Electron Spectrosc. Relat. Phenom.*, 150(2–3), 260–274, doi:10.1016/j.elspec.2005.06.008.

Lewis, E. R., and S. E. Schwartz (2004), *Sea Salt Aerosol Production: Mechanisms, Methods, Measurements and Models—A Critical Review*, *Geophys. Monogr. Ser.*, vol. 152, 413 pp., AGU, Washington, D. C., doi:10.1029/GM152.

Liu, Y., Z. Yang, Y. Desyaterik, P. L. Gassman, H. Wang, and A. Laskin (2008), Hygroscopic behavior of substrate-deposited particles studied by micro-FT-IR spectroscopy and complementary methods of particle analysis, *Anal. Chem.*, 80(3), 633–642, doi:10.1021/ac701638r.

Martens, C. S., J. J. Wesolows, R. C. Harriss, and R. Kaifer (1973), Chlorine loss from Puerto Rican and San Francisco Bay area marine aerosols, *J. Geophys. Res.*, 78(36), 8778–8792, doi:10.1029/JC078i036p08778.

Maskey, S., H. Geng, Y. C. Song, H. Hwang, Y. J. Yoon, K. H. Ahn, and C. U. Ro (2011), Single-particle characterization of summertime Antarctic aerosols collected at King George Island using quantitative energy-dispersive electron probe X-ray microanalysis and attenuated total reflection Fourier transform-infrared imaging techniques, *Environ. Sci. Technol.*, 45(15), 6275–6282, doi:10.1021/es200936m.

McInnes, L. M., D. S. Covert, P. K. Quinn, and M. S. Germani (1994), Measurements of chloride depletion and sulfur enrichment in individual sea-salt particles collected from the remote marine boundary layer, *J. Geophys. Res.*, 99(D4), 8257–8268, doi:10.1029/93JD03453.

Moffet, R. C., et al. (2008), Characterization of aerosols containing Zn, Pb, and Cl from an industrial region of Mexico City, *Environ. Sci. Technol.*, 42(19), 7091–7097, doi:10.1021/es7030483.

Moffet, R. C., A. V. Tivanski, and M. K. Gilles (2010a), Scanning X-ray transmission microscopy: Applications in atmospheric aerosol research, in *Fundamental Applications in Aerosol Spectroscopy*, edited by R. Signorell and J. P. Reid, pp. 419–462, Taylor and Francis, Philadelphia, Pa.

Moffet, R. C., T. R. Henn, A. Laskin, and M. K. Gilles (2010b), Automated chemical analysis of internally mixed aerosol particles using X-ray spectromicroscopy at the carbon K-edge, *Anal. Chem.*, 82(19), 7906–7914, doi:10.1021/ac1012909.

Mouri, H., and K. Okada (1993), Shattering and modification of sea-salt particles in the marine atmosphere, *Geophys. Res. Lett.*, 20(1), 49–52, doi:10.1029/92GL03004.

Mouri, H., I. Nagao, K. Okada, S. Koga, and H. Tanaka (1996), Elemental composition of individual aerosol particles collected from the coastal marine boundary layer, *J. Meteorol. Soc. Jpn.*, 74(5), 585–591.

Newberg, J. T., B. M. Matthew, and C. Anastasio (2005), Chloride and bromide depletions in sea-salt particles over the northeastern Pacific Ocean, *J. Geophys. Res.*, *110*, D06209, doi:10.1029/2004JD005446.

Pakkanen, T. A. (1996), Study of formation of coarse particle nitrate aerosol, *Atmos. Environ.*, *30*(14), 2475–2482, doi:10.1016/1352-2310(95)00492-0.

Pio, C. A., M. A. Cerqueira, L. M. Castro, and M. L. Salgueiro (1996), Sulphur and nitrogen compounds in variable marine/continental air masses at the southwest European coast, *Atmos. Environ.*, *30*(18), 3115–3127, doi:10.1016/1352-2310(96)00059-3.

Pósfai, M., J. R. Anderson, P. R. Buseck, T. W. Shattuck, and N. W. Tindale (1994), Constituents of a remote Pacific marine aerosol—A tem study, *Atmos. Environ.*, *28*(10), 1747–1756, doi:10.1016/1352-2310(94)90137-6.

Pósfai, M., J. R. Anderson, P. R. Buseck, and H. Sievering (1995), Compositional variations of sea-salt-mode aerosol particles from the North Atlantic, *J. Geophys. Res.*, *100*(D11), 23,063–23,074, doi:10.1029/95JD01636.

Prince, A. P., P. D. Kleiber, V. H. Grassian, and M. A. Young (2008), Reactive uptake of acetic acid on calcite and nitric acid reacted calcite aerosol in an environmental reaction chamber, *Phys. Chem. Chem. Phys.*, *10*(1), 142–152, doi:10.1039/b712915g.

Raemdonck, H., W. Maenhaut, and M. O. Andreae (1986), Chemistry of marine aerosol over the tropical and equatorial Pacific, *J. Geophys. Res.*, *91*(D8), 8623–8636, doi:10.1029/JD091iD08p08623.

Riedel, T. P., et al. (2012), Nitryl chloride and molecular chlorine in the coastal marine boundary layer, *Environ. Sci. Technol.*, doi:10.1021/es204632r, in press.

Ro, C. U., et al. (2001), Single-particle analysis of aerosols at Cheju Island, Korea, using low-Z electron probe X-ray microanalysis: A direct proof of nitrate formation from sea salts, *Environ. Sci. Technol.*, *35*(22), 4487–4494, doi:10.1021/es0155231.

Rossi, M. J. (2003), Heterogeneous reactions on salts, *Chem. Rev.*, *103*(12), 4823–4882, doi:10.1021/cr020507n.

Sarin, M., A. Kumar, B. Srinivas, A. K. Sudheer, and N. Rastogi (2010), Anthropogenic sulphate aerosols and large Cl-deficit in marine atmospheric boundary layer of tropical Bay of Bengal, *J. Atmos. Chem.*, *66*(1–2), 1–10, doi:10.1007/s10874-011-9188-z.

Shaw, G. E. (1991), Aerosol chemical components in Alaska air masses: 2. Sea salt and marine product, *J. Geophys. Res.*, *96*(D12), 22,369–22,372, doi:10.1029/91JD02059.

Sullivan, R. C., S. A. Guazzotti, D. A. Sodeman, Y. H. Tang, G. R. Carmichael, and K. A. Prather (2007), Mineral dust is a sink for chlorine in the marine boundary layer, *Atmos. Environ.*, *41*(34), 7166–7179, doi:10.1016/j.atmosenv.2007.05.047.

Yao, X. H., and L. M. Zhang (2012), Chemical processes in sea-salt chloride depletion observed at a Canadian rural coastal site, *Atmos. Environ.*, *46*, 189–194, doi:10.1016/j.atmosenv.2011.09.081.

Zaveri, R. A., et al. (2012), Overview of the 2010 Carbonaceous Aerosols and Radiative Effects Study (CARES), *Atmos. Chem. Phys. Discuss.*, *12*, 1299–1400, doi:10.5194/acpd-12-1299-2012.

Zhao, Y. L., and Y. Gao (2008), Acidic species and chloride depletion in coarse aerosol particles in the US east coast, *Sci. Total Environ.*, *407*(1), 541–547, doi:10.1016/j.scitotenv.2008.09.002.

Zhuang, H., C. K. Chan, M. Fang, and A. S. Wexler (1999), Formation of nitrate and non-sea-salt sulfate on coarse particles, *Atmos. Environ.*, *33*(26), 4223–4233, doi:10.1016/S1352-2310(99)00186-7.